



Preloaded behavior of thick one- way slabs strengthened with NSM –CFRP plates

Kutaiba A. Abbood^a, Raid A. Daud^{b*}

Dept. of Civil Engineering, College of Engineering, Al-Nahrain University, Iraq

^a M.Sc. Student , ^b Assist. Prof., Ph.D.,  Corresponding author, E-mail:

raid.a.daud@ced.nahrainuniv.edu.iq

8665

Abstract:

In this research, a nonlinear finite element model utilizing ABAQUS was adapted to obtain structural behavior of damaged one-way slabs and studies the influence of CFRP parameters and preloaded percentages to achieve better response. Three dimensional elements (solid, shell, truss) are used and the detailed model takes into consideration elastic and plastic behavior of the materials. The numerical outputs are validated with the authors' experimental data (monotonic and preloaded) to explore the precision of the model. Parametric studies using the validated model were conducted to investigate the effects of varying the bond length, the stiffness of CFRP (thickness & elastic modulus), the CFRP configurations and preloaded percentage. The preloaded numerical results showed that strengthening of damaged slabs using near surface mounted technique could be categorized as an effective, an economical and a successful approach.

KEYWORDS: strengthening, preloaded, NSM CFRP, thick One –Way Slabs.

DOI Number: 10.14704/nq.2022.20.6.NQ22858

NeuroQuantology 2022; 20(6): 8665-8679

1. Introduction

Strengthening of structures with Near- Surface Mounted Carbon Fiber Polymer (NSM FRP) is a method which has a considerable attention as a possible and effective instead of the method of strengthening structures with externally bonded FRP reinforcement (EBR). The former method shows some obvious advantages over the latter, due to NSM method shows better protection of the composite sheets from unexpected sources of damage

The increased use of composite material as a means of upgrading damaged structures is due to the desired characteristics of the composite material, specifically, excellent fatigue life, high corrosion resistance, low weight-to-strength ratio, etc. in addition, both the geometrical and material characteristics can be designed to fulfill the stiffness for any structural application [Raid A. Daud et al 2017] [1] [Ibrahim N. Najma et al 19][2] [Al-Azzawi 2017][3] .

[Fu-Ming et al 2004] [4] developed a numerical model for FRP-reinforced reinforced concrete structures. The proposed material models were checked to make sure they were correct. Fiber reinforcement has been shown to increase the stiffness and ultimate strength of reinforced concrete slabs by a large amount. By taking into account the different constitutive models, the authors came up with a good numerical model for analyzing reinforced concrete structures that were strengthened by FRP. If the longitudinal directions of the FRP line up with the yielding lines of RC slabs, the ultimate load of the slab might not go up too much. The best way to strengthen something is to make sure that the FRP's long direction and the direction of the most bending stress are parallel.

In [Gilles Foret a, Oualid Limam 2008] [5], showed that the NSM technique makes RC two-way slabs stronger. When compared to the EB technique, the NSM technique is also more



flexible. The NSM technique is more cost-effective because it uses less carbon fiber.

[Yail J. Kim et al 2015] [6] studied numerically the performance of pre-stress RC beams which were strengthened on the outside with post-tensioned by NSM CFRP strips. The focus was on design suggestions that would make it easier to use such a strengthening method in real life. Numerical simulations were done on 51 beam models to look at different mechanical features. The results showed that the cross-sectional areas of the draping bundle-strands ranged from 3561 mm² to 5941 mm² for the girders.

Fabric kinds and compressive strength of a concrete slab were explored by [Ali Hadi Adheem et al, 2018] [7] in order to determine how they affect the flexural performance in a reinforced RC slab, as well as how many fabric layers are necessary to achieve composite material effect. The results indicated that the reinforced slab bent differently depending on the type of fabric used. When the concrete strut failed and was crushed, the parametric investigation revealed that the flexural strength increased in tandem with the compressive strength. In addition, the RC slab's behavior was clearly affected by the composite material's amount of woven fabric, but only up to a certain point. This is due to the fact that the failure is depicted by the concrete's behavior in the compression side.

For his presentation, [Jose Ricardo Cruz et al 2020] [8] used numerical simulations to examine how reinforced concrete (RC) slabs enhanced with CFRP laminates placed by near surface mounting (NSM) and stiff and flexible adhesives fared in a flexural test. Bonding CFRP laminates with adhesive layers of varying stiffness (Young's module between 2.0% and 13.0% of Young's module) and deformability (final stresses between 0.20% and 150.0%) to

RC beams. Forces acting of up to 80.0% of the slabs' ultimate weight were applied during the loading procedure. Two factors were examined: There are two factors to consider: the adhesive type and the presence of pre-cracking in the slabs. The results indicated that the adhesive type had a significant impact on the flexural strength of the slab: 80.0 percent of the maximum load that can be reached with stiff adhesives can be accomplished with elastic adhesives. Pre-damage did not change how the slabs behaved structurally.

In [Sina Yazdani et al 2021] [9], a mathematical analysis of prestressed reinforced SCC slabs reinforced with externally bonded FRP composite systems (CFRP) sheets has been performed. There was a significant increase in load bearing capacity with an increase in the eccentricity ratio, but increasing concrete compressive strength and the use of more than two layers of CFRP had no effect. The results showed that the load bearing capacity and adaptability of reinforced SCC slabs may be significantly improved by combining the use of a single layer of CFRP sheet with prestressing. Because of this, the debonding of CFRP layers from concrete was inhibited when prestressing and CFRP strengthening procedures were utilized jointly.

In order to get an understanding of behavior of concrete slabs reinforced with carbon fiber-reinforced plastic (CFRP) bars, the effect of slab thickness was studied numerically [Mohammed A. Dheyab. Mu'taz K. Medhlom 2021] [10]. Three slabs with different thicknesses were modeled to observe the behavior. The samples were 1800 mm by 1800 mm and had thicknesses of 80, 130, and 180 mm. They were only held up by their corners. The results showed that the thickness of the slab is a controlling factor. Better performance



in slabs with CFRP bars is achieved by making the slabs stiffer.

The main objective of the current study is to present numerically an obvious understanding of how the preloaded structural behavior of thick one way slabs is influenced by the CFRP parameters and preloaded percentage.

2. Methodology for numerical simulation

2.1 Numerical simulation model

The general numerical program package ABAQUS was utilized to present the actual model. Concrete was modeled using (C3D8R) the isoperimetric eight-node brick element. Every node has three-dimensional movements in x, y and z directions. While for reinforced steel rebars, the three-dimensional two-node bar element with three-dimensional movements, truss element (T3D2) was selected,

and to represent the CFRP plate three dimensional 4-node with reduced integration and hourglass control (S4R5) was used. For each slab, two-line load was subjected at the top of the slab as uniform pressure with the same area and position of experimental test . Displacement boundary conditions was used for modeling end supports of model, to properly simulated the analytical model similar to that of the tested slabs, the boundary conditions required to be utilized at the points that are used to support the specimens in experiments test. Since the specimens were simply supported over the two shorter edges, all the nodes along one of the supporting lines were the fixed translated in y and z-direction, and one the other supported line was fixed translated in x, y and z-direction as illustrated in **Figure 1**

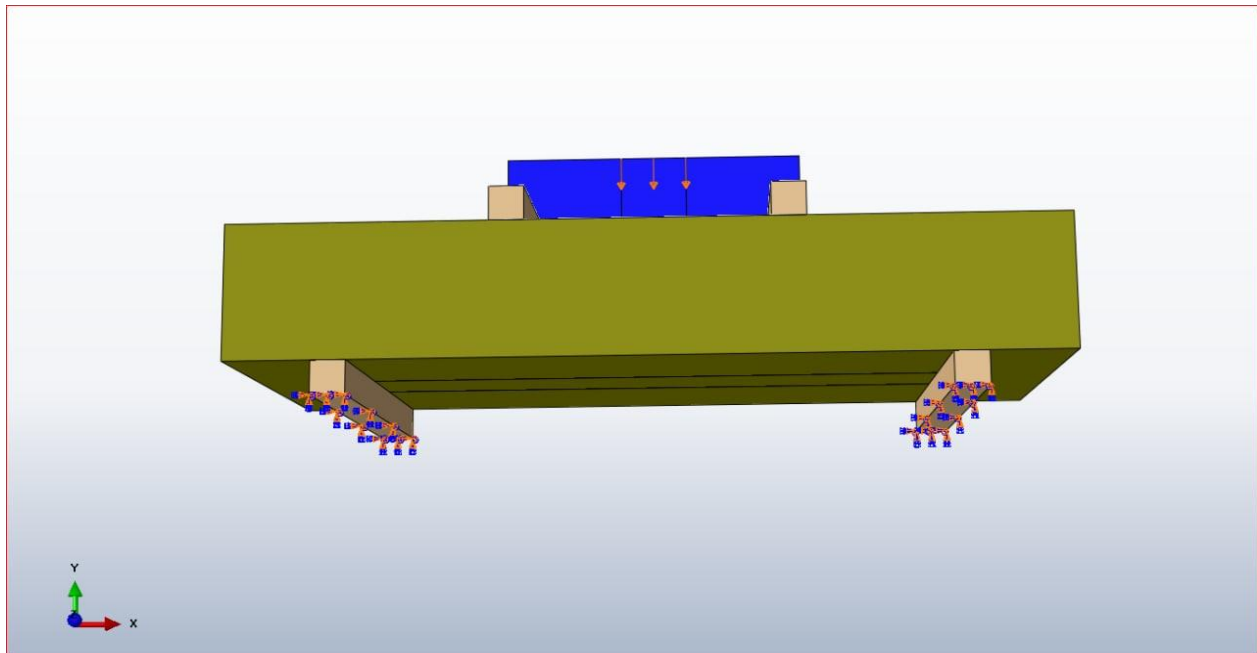


Figure 1: Isometric view of applied load and boundary condition for ends supports.

2.2. Material models

2.2.1 Concrete

The concrete damaged plasticity model (CDP) was developed using [Lubliner et al][11] yield function. Tensile cracking and compression fractures are the two types of failure processes that this model incorporates. The CDP is a well-known model that is used to describe the behavior of concrete. It is also utilized for the nonlinear computation of concrete members due to the fact that it provides an excellent explanation of behavior of the material [J. S. Tyau] [12]. Table (1) shows input data for concrete damage plasticity parameters

2.2.1.1 Concrete Compressive Behavior

Concrete has high compressive strength and the elastic linear path is about 40 % of total compressive strength and non- linear is started because the appearance of cracks. Both ascending and strain descending ranges are specified by ABAQUS in terms of concrete stress σ_c and inelastic concrete strain, respectively. The model of [BSI-2004] Euro code two design of concrete structure [13] was conducted in the current finite element analysis. Table (2) shows concrete compressive strength data

2.2.1.2 Concrete Tensile Behavior

In ABAQUS/standard, there are three ways to describe the post-cracking tension softening

curve: strain, displacement, or fracture energy. In the current analysis, the tensile stress-strain curve of concrete was provided in ABAQUS to involve a linear rising line with gradient equal to the elastic modulus of concrete and exponential sliding derived by [Wang and Hsu (2001)][14]. Table (3) shows concrete tension data

2.2.2 Steel Reinforcement

The steel reinforcement behavior was modeled in ABAQUS as a bilinear elastic-plastic curve. The linear elastic zone of the behavior was modeled by the elastic modulus and Poisson's ratio, while the plastic curve was obtained from experimental data of stress-strain curve. Table (4) illustrates the properties of steel reinforcement

2.2.3 Carbon Fiber Reinforced Polymer (CFRP)

The CFRP composite plate was modeled as an orthotropic material. It has linear behavior to the end of failure. The elastic main modulus in the longitudinal direction was written according to the manufacture data, with the other two transverse elastic moduli assumed as about ten percent of the elastic main modulus. Other properties were assumed according to those specified by [Reddy][15]. Table (5) illustrates the elastic properties of CRP Plates

Table 1: Input data for concrete damage plasticity parameters.

| | |
|-------------------------------|-------------|
| Young's modulus | 32036.35475 |
| Poisson ratio | 0.15 |
| Dilation angle | 36 |
| Eccentricity | 0.1 |
| $\epsilon_{bo}/\epsilon_{co}$ | 1.16 |
| k_c | 0.667 |
| Viscosity parameter | 0 |

Table 2: Concrete compressive strength

| Yield Stress (MPa) | Inelastic Strain |
|---------------------------|-------------------------|
| 6.931126884 | 0 |
| 18.35027156 | 8.28E-05 |
| 26.66728606 | 0.000260183 |
| 32.05637537 | 0.000529001 |
| 34.67894046 | 0.000884175 |
| 35 | 0.001092671 |
| 34.46516115 | 0.001394373 |
| 32.88545768 | 0.001728689 |
| 30.29682902 | 0.002094499 |
| 26.73358503 | 0.00249073 |
| 22.22849735 | 0.002916361 |

Table 3: Concrete tension data

| Yield Stress (MPa) | Strain |
|---------------------------|---------------|
| 3.26 | 0 |
| 0.330471049 | 0.031091444 |

Table 4: Properties of steel reinforcement

| | |
|----------------------|---------------------|
| fy | 524 (MPa) |
| fu | 650 (MPa) |
| Poisson ratio | 0.3 |
| Es | 200000 (MPa) |
| elongation | 15% |



Table 5:elastic Properties of CFRP Plate[Reddy][14].

| Material | Description | CFRP plate |
|------------|---|------------|
| CFRP plate | Longitudinal modulus (E1), GPa | 160 |
| | Transverse in-plane modulus(E2), GPa | 160 |
| | Transverse out-plane modulus(E3), GPa | 160 |
| | In- plane shear modulus (G12), GPa | 6.894 |
| | out- of-plane shear modulus (G23), GPa | 4.136 |
| | out- of-plane shear modulus(G13),GPa | 6.894 |
| | Major in -plane Passion's ratio, ν_{12} | 0.3 |
| | Out-of-plane Passion's ratio, ν_{23} | 0.25 |
| | Out-of-plane Passion's ratio, ν_{13} | 0.25 |

*E₁ value taken from manufacture CFRP information

3 Predefined field

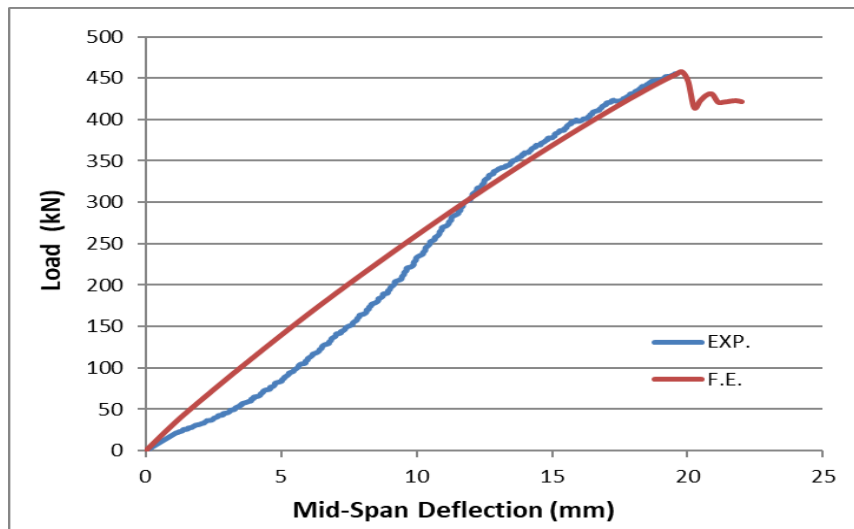
ABAQUS/ Standard suggest method to define preloaded stage of damaged slabs. This method named predefined field which is presented by initial state field. It can be linked to any component instance in an ABAQUS/CAE model using data imported from a previous ABAQUS/Standard model results, and the job name associated with the analysis from which the initial state field is imported, can be specified at particular step and increment of the analysis from an imported ABAQUS/CAE model data. Even more importantly, findings and model information may be moved to a new study where you can define additional model definitions before proceeding with the analysis in ABAQUS/Standard. In this study, for specimens with CFRP plates, this capability allows 70 percent of the ultimate load to be applied and to use the deformed model

associated with the material condition as an initial state.

4 Validation of Finite Element Simulation Model

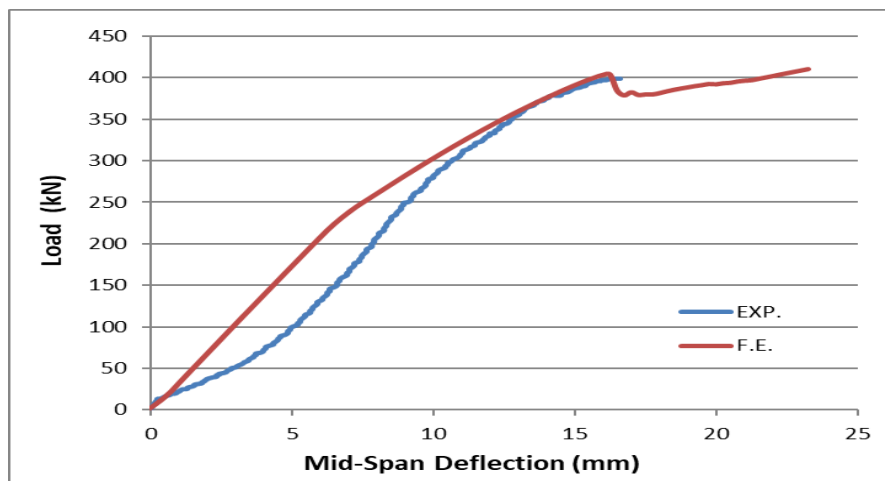
This section contains comparisons to the experimental outcomes. These include the load-deflection relationship when a pressure load is applied after repairing the slabs, as well as (load and deflection) at the ultimate stage when preloads and monotonic loads are applied. **Figure 2** shows a comparison in load versus deflection relation between the experimental and numerical results for monotonic load test after repairing the damaged slabs. It could be demonstrated that finite element outcomes were stiffer than test results for linear and non-linear behavior domains, with reasonable agreement.





(MS)

* slab Under monotonic load without strengthening



(PSS)

*slab under preloaded without strengthening

Figure 2 Comparison between simulation and experimental results

Table 6 illustrates comparisons between the ultimate load and central deflection extracted from numerical model and the test at final stage (nearby failure load) for all slabs under monotonic load. Reasonable agreement was acquired between ultimate load and deflections of FE models and that found experimentally where, the value for $(P_u)_{FE}/(P_u)_{Exp}$ 1.004 and 1.008 respectively for ultimate loads, whilst, for the deflection $(\delta_{FE} / \delta_{Exp})$ 1.121 and 1.222 respectively as shown in the table **Table 6**

Table 6 : Experimental and numerical ultimate load and deflection at failure load.

| SLAB labeling | Ultimate Load kN | | $(P_u)_{FE}/(P_u)_{Exp}$ | deflection (mm) | | δ_{FE}/δ_{Exp} |
|---------------|------------------|--------------|--------------------------|------------------|---------------|----------------------------|
| | $(P_u)_{Exp}$ | $(P_u)_{FE}$ | | δ_{Exp} | δ_{FE} | |
| MS | 455.16 | 457.013 | 1.004 | 19.63 | 22 | 1.121 |
| PSS | 433.59 | 436.907 | 1.008 | 19.03 | 23.25 | 1.222 |

* MS: slab without damage , PSS: damaged slab by preloaded 70% of the ultimate load

The results of the finite element analysis (load-deflection relationship under applied load) indicate that the models are stiffer than the experimental specimens. There are several factors that might account for the increased stiffness shown in FEM study findings. Micro-cracks in the concrete are discovered during the experiment as a result of drying shrinkage and curing. These would result in a reduction in the specimen's true stiffness. These micro-cracks are not modeled in finite element models. In numerical analysis, the connection between steel bar and concrete is considered to be tie. This assumption will not be entirely accurate in the case of the tested specimen. When a bond slip occurs, composite action between the steel and concrete is lost. As a result, the total stiffness of the actual specimen may be less than predicted by FE analysis [K. Hibbitt and I. Sorensen] [16].

5 Numerical Parametric Studies

Based on the previous finite element verification for the experimental data carried out during this study, an extensive parametric analysis was conducted by using the finite element model. The investigation parameters are the effect of thickness of added CFRP, the effect of modulus of elasticity of added CFRP,

the effect of distribution of added CFRP strips, and the effect of preload value on the structural performance of damaged slabs under monotonic load.

5.1 Effect of added CFRP thickness on structural performance of slabs

The influence of added CFRP thickness on failure load and load- mid span deflection relation was studied for slabs. Three thickness values were chosen (1.2, 2.4, and 3.6 mm) each thickness with three slabs based on the length of CFRP strip where three lengths were chosen (600, 800, and 1000mm). It is clear that the increase in adding CFRP strips' thickness increased the stiffness of slabs, which led to an increase in the failure load whatever value of strip length. **Table 7** shows that the percent of the increase in ultimate load capacity is 10.4, and 15.5% for slab S1000-2.4 and S1000-3.6, respectively related to slab S1000-1.2 for group of CFRP length = 1000mm, while the percent of the increase in ultimate load capacity is 8.9, and 13% for slab S800-2.4 and S800-3.6, respectively related to slab S800-1.2 for group of CFRP length = 800mm. The percent of the increase in ultimate load capacity is 2.1, and 2.15% for slab S600-2.4 and S600-3.6, respectively related to slab S600-1.2 for group of CFRP length = 600mm. **Figure 3** shows the effect of added CFRP thickness and length on ultimate load capacity.



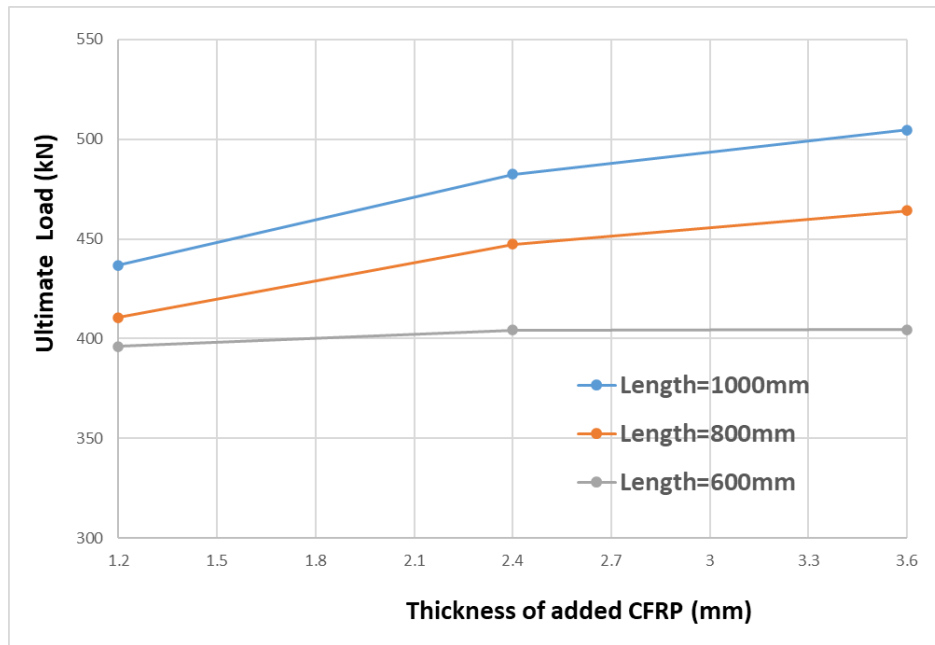


Figure 3: Effect of CFRP thickness and length on ultimate load capacity.

Table 7: Effect of added CFRP thickness on ultimate load capacity.

| SLAB ID | CFRP length (mm) | CFRP thickness (mm) | $P_u = P_{ult.}$ (kN) | Increase percent of P_u related to P_u of (1.2mm in each group) (%) |
|-----------|------------------|---------------------|-----------------------|---|
| S1000-1.2 | 1000 | 1.2 | 436.91 | Ref. |
| S1000-2.4 | 1000 | 2.4 | 482.45 | 10.4 |
| S1000-3.6 | 1000 | 3.6 | 504.76 | 15.5 |
| S800-1.2 | 800 | 1.2 | 410.6 | Ref. |
| S800-2.4 | 800 | 2.4 | 447.27 | 8.9 |
| S800-3.6 | 800 | 3.6 | 464.09 | 13 |
| S600-1.2 | 600 | 1.2 | 395.965 | Ref. |
| S600-2.4 | 600 | 2.4 | 404.283 | 2.1 |
| S600-3.6 | 600 | 3.6 | 404.47 | 2.15 |

5.2 Effect of added CFRP modulus of elasticity on structural performance of slabs

The effect of modulus of elasticity of added CFRP on ultimate load capacity and load-deflection relation was studied for slabs. Three modulus of elasticity values were chosen (160, 240, and 640 GPa). It is clear that the increase in adding CFRP strips' modulus of elasticity increased the stiffness of slabs, which led to an increase in the ultimate load whatever the value of the strip length. Also, the increase in adding CFRP strips' length increased the stiffness of slabs, which led to an increase in the ultimate load.



Table 8 shows that the percent of the increase in ultimate load capacity is 1.5, and 13.3% for slab S1000-240 and S1000-640, respectively related to slab S1000-160 for group of CFRP length = 1000mm, while the percent of the increase in ultimate load capacity is 4.1, and 14.3% for slab S800-240 and S800-640, respectively related to slab S800-160 for group of CFRP length = 800 mm. The percent of the increase in ultimate load capacity is 1.5, and 2.3% for slab S600-240 and S600-640, respectively related to slab S600-160 for group of CFRP length = 600 mm. **figure 4** shows the effect of modulus of elasticity and length of added CFRP strips on ultimate load capacity.

Table 8: Effect of modulus of elasticity and length of added CFRP on ultimate load capacity.

| SLAB ID | CFRP width (mm) | CFRP length (mm) | CFRP modulus of elasticity (GPa) | Pu=P _{ultimate} (kN) | Increase percent of Pu related to Pu of (160 GPa in each group) (%) |
|-----------|-----------------|------------------|----------------------------------|-------------------------------|---|
| S1000-160 | 30 | 1000 | 160 | 436.91 | Ref. |
| S1000-240 | 30 | 1000 | 240 | 443.57 | 1.5 |
| S1000-640 | 30 | 1000 | 640 | 495.2 | 13.3 |
| S800-160 | 30 | 800 | 160 | 410.6 | Ref. |
| S800-240 | 30 | 800 | 240 | 427.278 | 4.1 |
| S800-640 | 30 | 800 | 640 | 469.144 | 14.3 |
| S600-160 | 30 | 600 | 160 | 395.965 | Ref. |
| S600-240 | 30 | 600 | 240 | 401.942 | 1.5 |
| S600-640 | 30 | 600 | 640 | 405.211 | 2.3 |

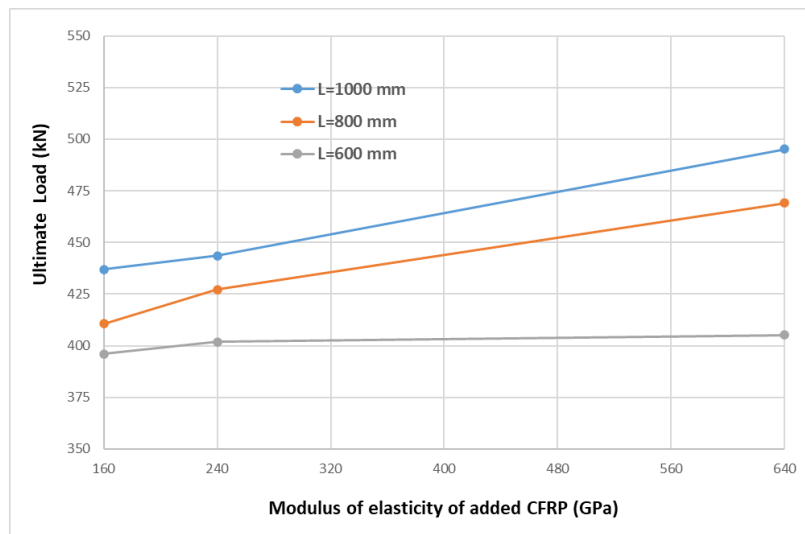


Figure 4: Effect of modulus of elasticity and length of added CFRP strips on ultimate load capacity, (width=30 mm for all).



5.3 Effect of added CFRP configuration on structural performance of slabs

the effect of distribution and length of added CFRP strips on slabs' load-mid span deflection relation. It is clear that the increase in adding CFRP strips' numbers increased the stiffness of slabs, which led to an increase in the ultimate load whatever value of strip length. Also, the increase in adding CFRP strips' length increased the stiffness of slabs, which led to an increase in the ultimate load.

Table 9 shows that the percent of the increase in ultimate load capacity is 3.9, 11.1, and 13.7%

for slab S1000-3, S1000-4, and S1000-5, respectively related to slab S1000-2 for group of CFRP length = 1000mm, while the percent of the increase in ultimate load capacity is 5.8, 8.7, and 10.9% for slab S800-3, S800-4, and S800-5, respectively related to slab S800-2 for group of CFRP length = 800mm. The percent of the increase in ultimate load is 2.3, 3.3, and 3.7% for slab S600-3, S600-4, and S600-5, respectively related to slab S600-2 for group of CFRP length = 600mm. **Figure 5** shows the influence of configuration and added CFRP strips length on ultimate load.

Table 9: Effect CFRP configuration of different length on ultimate load capacity.

| SLAB ID | No. of CFRP strips | CFRP length (mm) | Pu=P _{ultimate} (kN) | Increase percent of Pu related to Pu of (2-strips in each group) (%) |
|---------|--------------------|------------------|-------------------------------|--|
| S1000-2 | 2 | 1000 | 436.91 | Ref. |
| S1000-3 | 3 | 1000 | 453.89 | 3.9 |
| S1000-4 | 4 | 1000 | 485.53 | 11.1 |
| S1000-5 | 5 | 1000 | 496.55 | 13.7 |
| S800-2 | 2 | 800 | 410.6 | Ref. |
| S800-3 | 3 | 800 | 434.3 | 5.8 |
| S800-4 | 4 | 800 | 446.37 | 8.7 |
| S800-5 | 5 | 800 | 455.23 | 10.9 |
| S600-2 | 2 | 600 | 395.97 | Ref. |
| S600-3 | 3 | 600 | 404.997 | 2.3 |
| S600-4 | 4 | 600 | 408.919 | 3.3 |
| S600-5 | 5 | 600 | 410.495 | 3.7 |



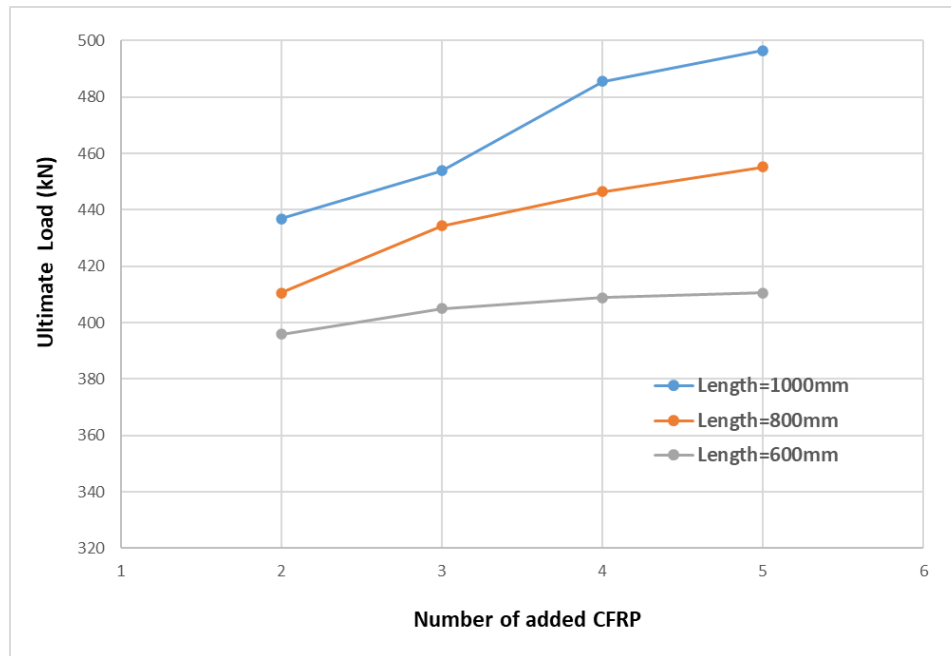


Figure 5: Effect of distribution and length of CFRP strips on ultimate load.

5.4 Effect of preload percent on structural performance of slabs

a comparison between strengthened and un-strengthened slabs for three preload percents of the ultimate load (60, 70, and 80%) in load-mid span deflection relationship. the effect of preload on slabs' load-mid span deflection relation. It is clear that the increase in adding CFRP strips' numbers increased the stiffness of slabs, which led to an increase in the ultimate load whatever the value of the strip length. Also, the increase in adding CFRP strips' length increased the stiffness of slabs, which led to an increase in the ultimate load capacity. It is clear that the increase in preload percent decreased the stiffness of slabs, which led to a decrease in

the ultimate load. Knowing that the strengthened slabs are strengthened with CFRP with a length of 1000 mm and a width of 30 mm.

Table 10 shows that the percent of the decrease in ultimate load capacity is 0.7, and 5.7% for slab S70, and S80, respectively related to slab S60 for group of un-strengthened slabs, while the percent of the decrease in ultimate load capacity is 0.46, and 4.65% for slab SS70, and SS80, respectively related to slab SS60 for group of strengthened slabs. **Figure 6** shows the effect of preload percent on ultimate load capacity.



Table 10: Effect of preload presents on ultimate load capacity.

| Group | Beam ID | preload presents (%) | CFRP dimensions (mm) | $P_u = P_{ultimate}$ (kN) | Decrease percent of P_u related to P_u of (60% in each group) (%) |
|-----------------|---------|----------------------|----------------------|---------------------------|---|
| un-strengthened | S60 | 60 | - | 364.1 | Ref. |
| | S70 | 70 | - | 361.7 | 0.7 |
| | S80 | 80 | - | 343.5 | 5.7 |
| Strengthened | SS60 | 60 | 1000x30 | 436.9 | Ref. |
| | SS70 | 70 | 1000x30 | 434.9 | 0.46 |
| | SS80 | 80 | 1000x30 | 416.6 | 4.65 |

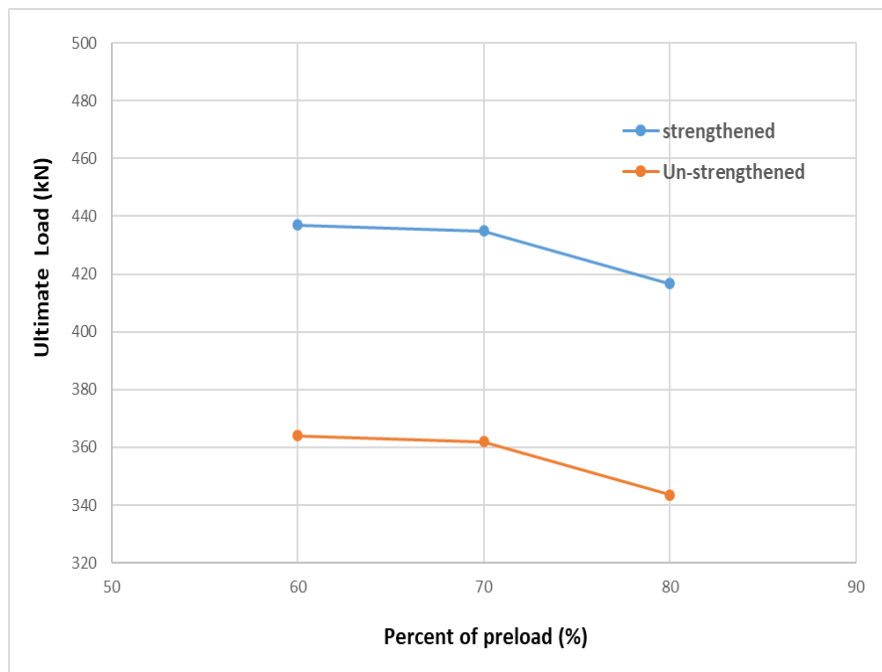


Figure 6: Effect of preload presents on ultimate load capacity.

6 Conclusions based on numerical results

- Reasonable agreement was acquired between failure loads and deflections of FE numerical model and that found by test in which the value of the average and coefficient of variations for $(P_u)_{FE}/(P_u)_{Exp}$ were 1.122 and 24.94 %, respectively for ultimate

loads, whilst, for the deflection ($\delta_{FE} / \delta_{Exp}$) the value of the average, and coefficient of variation were 1.421 and 23.93 %, respectively.

- The influence of CFRP thickness on ultimate load was studied numerically, the percent of the increase in ultimate load is 10.4, and 15.5% for slab S1000-



2.4 and S1000-3.6, respectively related to slab S1000-1.2 for group of CFRP length = 1000mm, while the percent of the increase in ultimate load capacity is 8.9, and 13% for slab S800-2.4 and S800-3.6, respectively related to slab S800-1.2 for group of CFRP length = 800mm. The percent of the increase in ultimate load capacity is 2.1, and 2.15% for slab S600-2.4 and S600-3.6, respectively related to slab S600-1.2 for group of CFRP length = 600mm.

3- The effect of CFRP modulus of elasticity on ultimate load capacity was studied numerically. The percent of the increase in ultimate load capacity is 1.5, and 13.3% for slab S1000-240 and S1000-640, respectively related to slab S1000-160 for group of CFRP length = 1000mm, while the percent of the increase in ultimate load capacity is 4.1, and 14.3% for slab S800-240 and S800-640, respectively related to slab S800-160 for group of CFRP length = 800 mm. The percent of the increase in ultimate load capacity is 1.5, and 2.3% for slab S600-240 and S600-640, respectively related to slab S600-160 for group of CFRP length = 600 mm

4- The effect of CFRP distribution on ultimate load capacity was studied numerically, the percent of the increase in ultimate load capacity is 3.9, 11.1, and 13.7% for slab S1000-3, S1000-4, and S1000-5, respectively related to slab S1000-2 for group of CFRP length = 1000mm, while the percent of the increase in ultimate load capacity is 5.8, 8.7,

and 10.9% for slab S800-3, S800-4, and S800-5, respectively related to slab S800-2 for group of CFRP length = 800mm. The percent of the increase in ultimate load is 2.3, 3.3, and 3.7% for slab S600-3, S600-4, and S600-5, respectively related to slab S600-2 for group of CFRP length = 600mm.

5- The effect of preload percent on structural performance of slabs was studied numerically, the increase in preload percent decreased the stiffness of slabs, which led to a decrease in the ultimate load. Knowing that the strengthened slabs are strengthened with CFRP with a length of 1000 mm and a width of 30 mm. The percent of the decrease in ultimate load capacity is 0.7, and 5.7% for slab S70, and S80, respectively related to slab S60 (preload percent=60% of P_u) for group of unstrengthened slabs, while the percent of the decrease in ultimate load capacity is 0.46, and 4.65% for slab SS70, and SS80, respectively related to slab SS60 for group of strengthened slabs.

ACKNOWLEDGMENT

The authors would like to thank Al-Nahrain University for support this work.

REFERENCES

- 1-Daud, Raid A., Lee S. Cunningham, and Yong C. Wang. "New model for post-fatigue behaviour of CFRP to concrete bond interface in single shear." *Composite Structures* 163 (2017): 63-76.
- 2-Najm, I. N., Daud, R. A., & Al-Azzawi, A. A. (2019). Behavior of reinforced concrete segmental hollow core slabs under monotonic and repeated loadings. *Structural Monitoring and Maintenance*, 6(4), 269-289.



- 3- Al-Azzawi, A. A. (2017). Free vibration of simply supported beam on elastic foundations. *Al-Nahrain Journal for Engineering Sciences*, 20(2), 353-357.
- 4- Lin, F. M., & Hu, H. T. (2004, May). Strengthening of Square Reinforced Concrete Plates with Fiber Reinforced Plastics. In *The Fourteenth International Offshore and Polar Engineering Conference*. OnePetro.
- 5- Foret, G., & Limam, O. (2008). Experimental and numerical analysis of RC two-way slabs strengthened with NSM CFRP rods. *Construction and Building Materials*, 22(10), 2025-2030.
- 6-Kim, Y. J., Kang, J. Y., & Park, J. S. (2015). Post-tensioned NSM CFRP strips for strengthening PC beams: A numerical investigation. *Engineering Structures*, 105, 37-47.
- 7-Adheem, A. H., Ali, I. M., & Shaker, M. S. (2018). Flexural Behavior of RC One-Way Slabs Strengthened with Fiber Reinforcement Cementations Matrix, FRCM. *Journal of University of Babylon for Engineering Sciences*, 26(10), 23-35.
- 8- Cruz, J. R., Seręga, S., Sena-Cruz, J., Pereira, E., Kwiecień, A., & Zajac, B. (2020). Flexural behaviour of NSM CFRP laminate strip systems in concrete using stiff and flexible adhesives. *Composites Part B: Engineering*, 195, 108042.
- 9-Yazdani, S., Asadollahi, S., Shoaee, P., & Dehestani, M. (2021). Failure stages in post-tensioned reinforced self-consolidating concrete slab strengthened with CFRP layers. *Engineering Failure Analysis*, 122, 105219.
- 10-Dheyab, M. A., & Mu'taz, K. (2021). NUMERICAL EVALUATION OF SLAB THICKNESS EFFECT ON THE IMPACT BEHAVIOR OF CONCRETE SLABS REINFORCED WITH CFRP BARS. *Journal of Engineering and Sustainable Development (JEASD)*, 25(Special_Issue_2021).
- 11- J. Lubliner, J. Oliver, S. Oller, and E. Oñate, "A plastic-damage model for concrete," *Int. J. Solids Struct.*, vol. 25, no. 3, pp. 299–326, 1989.
- 12-J. S. Tyau, "Finite element modeling of reinforced concrete using 3-dimensional solid elements with discrete rebar," Master Sci. Dept. Civ. Environ. Eng. Brigham Young Univ, 2009.
- 13-British Standards Institutio Eurocode 2: Design of concrete structures: Part 1-1: General rules and rules for buildings. British Standards Institution,2004.
- 14- Wang, T., & Hsu, T. T. (2001). Nonlinear finite element analysis of concrete structures using new constitutive models. *Computers & structures*, 79(32), 2781-2791.
- 15- Reddy JN. *Mechanics of laminated composite plates and shells: theory and analysis*. CRC Press; 2004.
- 16- K. Hibbitt and I. Sorensen, "ABAQUS/Standard User's Manual Volumes I-III and ABAQUS CAE Manual." Version, 2014.

